



Cite this: *Environ. Sci.: Water Res. Technol.*, 2022, 8, 957

## Emerging investigator series: effects of sediment particle size on the spatial distributions of contaminants and bacterial communities in the reservoir sediments

Wenbin Chen,<sup>a</sup> Ying Wang,<sup>b</sup> Leigang Wang,<sup>c</sup> Yu Ji,<sup>a</sup> Qilin Wang,<sup>d</sup> Ming Li <sup>a</sup> and Li Gao <sup>\*e</sup>

Natural sediment deposition can affect the storage capacity and water supply reliability of the reservoir, which could be resolved effectively by desilting. The successful implementation of partial desilting requires a thorough understanding of the spatial distribution of the contaminants and bacterial communities in the reservoir sediments. In this study, the effects of sediment particle size on the spatial distribution of contaminants and bacterial communities in the reservoir sediments were investigated. It was identified that the surface sediment particle size of the Linghe Reservoir firstly reduced from the reservoir head to center of the reservoir and then increased to the highest value at the backwater area. The contents of total nitrogen (TN), total phosphorus (TP), organic matter (OM) and soluble organic carbon in sediments were negatively correlated with the sediment particle size. It was found that moderate Cd contamination existed in the Linghe Reservoir, however, no other heavy metal (Pb, Cu, Zn, Cr, Mn, and Ni) contamination was identified. There was also no significant correlation between spatial distribution of heavy metals and the sediment particle size. The horizontal difference in sediment particle size also indirectly affected the bacterial community structure and the dissolved organic matter (DOM) content released by the bacteria. This study clearly shows that the horizontal difference in flow velocity led to the natural horizontal distribution of sediment particle size, which further directly affected the horizontal distributions of organic carbon, nitrogen and phosphorus and indirectly affected bacterial community structure and the DOM content released by the bacteria in the sediments.

Received 26th November 2021,  
Accepted 18th March 2022

DOI: 10.1039/d1ew00877c

rsc.li/es-water

### Water impact

The partial desilting is considered as a cost-effective approach to improve the water quality and partially increase the storage capacity of the reservoir. This study investigates the effects of sediment particle size on the spatial distributions of contaminants and bacterial communities in the reservoir sediments, which can facilitate and guide the implementation of partial desilting in the reservoirs.

## 1. Introduction

The man-made reservoir is an important measure to effectively regulate and utilize water resources.<sup>1</sup> Natural

sediment deposition is one of the key reservoir operational problems, especially for the small to medium sized reservoirs.<sup>2</sup> It is estimated that the sediment deposition has resulted in an annual loss of 0.5–1.0% of the total reservoir capacity worldwide, which is higher than the annual increase of storage capacity by new-built reservoirs.<sup>3</sup> In addition, the sediment deposition usually contains various nutrients and contaminants, which can cause water quality deterioration in the reservoirs, and subsequently, affect the water supply security.<sup>4</sup>

Desilting is one of the main approaches to resolve the above reservoir operational problems. However, the whole reservoir desilting can be cost prohibitive, since the cost is often higher than the capital investment of a new reservoir.

<sup>a</sup> College of Natural Resources and Environment, Northwest A & F University, Yangling 712100, PR China

<sup>b</sup> Shaanxi Province Institute of Resources and Electric Power Investigation and Design, Xi'an 710613, PR China

<sup>c</sup> PowerChina Northwest Engineering Corporation Limited, Xi'an 710065, PR China

<sup>d</sup> Centre for Technology in Water and Wastewater, School of Civil and Environmental Engineering, University of Technology Sydney, Ultimo, NSW 2007, Australia

<sup>e</sup> Institute for Sustainable Industries and Liveable Cities, Victoria University, PO Box 14428, Melbourne, Victoria 8001, Australia. E-mail: li.gao@sew.com.au

The partial desilting is considered as a compromise approach. It is more cost-effective and can significantly improve the water quality and partially increase the storage capacity of the reservoir. The successful implementation of partial desilting requires a thorough understanding of the spatial distribution of the contaminants and bacterial communities in the reservoir sediments, which is highly dependent on the sediment particle size.

When water flows into a reservoir, the flow velocity will gradually decrease, leading to the sedimentation of particles carried by the water. This natural sedimentation process will result in the large particle deposition in the backwater area of the reservoir tail, while the small particles will deposit in the center of the reservoir.<sup>5</sup> In the reservoir head, the size of deposited particles is relatively large due to the periodic water flushing by the floods. Consequently, there exists a natural spatial distribution of the sediment particle size in the reservoir. Generally, the smaller particles have the larger specific surface area and better adsorption capacity.<sup>6</sup> Therefore, the natural spatial distribution of sediment particle size will inevitably affect the contaminants distribution in the reservoir sediments.

Researchers have undertaken field studies to investigate the spatial distribution of contaminants in the reservoir sediments. Mwanamoki *et al.*<sup>7</sup> have investigated the trace metals and persistent organic pollutants (POPs) in the sediments of the Lake Ma Vallee at the Democratic Republic of Congo. They found that there was a correlation between the median sediment particle size and the physico-chemical properties of the sediments. Other studies<sup>8–10</sup> have also suggested that the sediments in the backwater area or the head of the reservoir generally contain significantly higher heavy metal contents compared to the sediments from the reservoir center.

Sediment particle size is considered as an important factor affecting the spatial distribution of contaminants.<sup>11–13</sup> In addition, previous studies<sup>14–16</sup> have demonstrated that sediment particle size plays an essential role in determining the bacterial abundance and community structure, which subsequently affects the biodegradation of the contaminants. A better insight into the effects of sediment particle size on spatial distribution of the contaminants and bacterial communities in the reservoir sediments can facilitate the successful implementation of the partial desilting.

Linghe Reservoir is located in Lintong District at Xi'an city, Shaanxi Province. Its surface area and total capacity are approximately 1 million m<sup>2</sup> and 39.9 million m<sup>3</sup>, respectively. This medium-sized reservoir is built mainly for the irrigation purpose, but is also utilized for flood control and fish farming. Linghe River flows through the ecologically fragile Loess Plateau, where intensive soil erosion occurs. Therefore, the river carries a large amount of sediments, which finally deposit in the Linghe Reservoir. Currently, the average depth of Linghe Reservoir has reduced to less than 3 m, which has significantly affected the reservoir storage capacity and water supply security. The above features allow the Linghe

Reservoir as a desired site to study the effects of sediment particle size on the spatial distributions of the contaminants and bacterial communities in the sediments.

## 2. Materials and methods

### 2.1. Study site

In this study, the Linghe Reservoir was divided into four sections based on the distance from the dam. Section A is located at the reservoir head, and section D is located in the backwater area of the reservoir tail (Fig. 1). Three samples were collected from each section.

### 2.2. Sample collection

Surface sediments (0–15 cm depth) were collected at each site by the Peterson grab sampler from the Linghe Reservoir in November 2020. The sediment samples (1 L) were firstly sealed in the labeled polyethylene plastic boxes. They were then stored in the car refrigerator and transported to the laboratory immediately after the sampling. The fresh sediment samples were divided into three parts. The first part was used for the sediment particle size analysis; the second part was naturally dried at room temperature, afterwards, it was milled by an agate pestle and mortar and filtered through a 150 µm sieve for the subsequent chemical analysis; the final part was stored at –80 °C for the following bacterial DNA extraction.

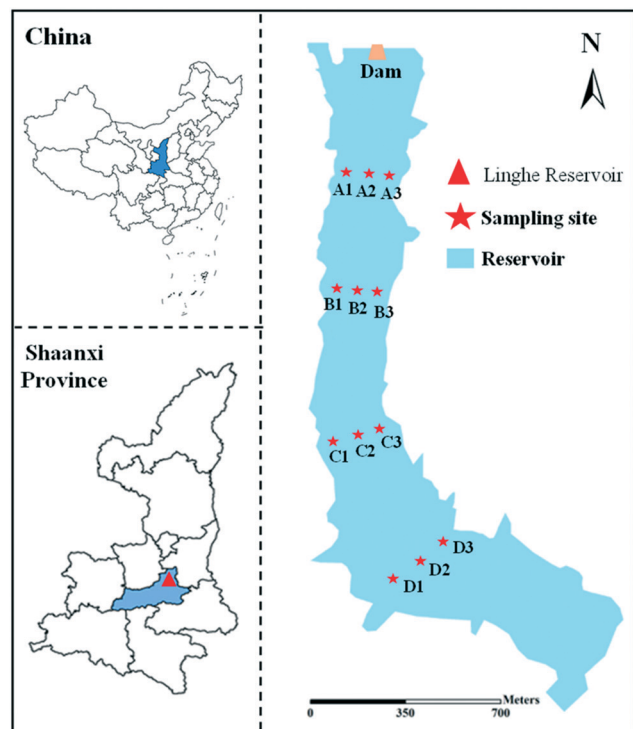


Fig. 1 Location of the Linghe Reservoir and 12 sampling sites.

### 2.3. Analytical methods

**2.3.1. Particle size analysis.** To determine the grain size distribution, fresh sediment samples were firstly treated by H<sub>2</sub>O<sub>2</sub> (10% w/w) to remove the organic matters. The samples were then disaggregated and dispersed ultrasonically with pyrophosphate.<sup>17</sup> Sediment particle size was measured using a particle size analyzer (Mastersizer 2000 particle size analyzer, Malvern Instruments, UK), which has been used extensively for analyzing various types of particles.<sup>18,19</sup> In this study, D<sub>50</sub> was used to characterize the overall spatial distribution of sediments with different particle sizes. Here, D<sub>50</sub> refers to the particle size when the cumulative percentage of particle size distribution reaches 50%.

**2.3.2. Chemical analysis.** Standard methods<sup>20</sup> were used to determine the TN, TP and OM in sediment samples. The soluble organic carbon was measured by a total organic carbon analyzer (TOC-L, Shimadzu, Japan). The fluorescence excitation–emission matrices (EEMs) spectra of DOM in the sediment samples were analyzed by a fluorescence spectrometer (RF-6000, Shimadzu, Japan). The fluorescence spectrum of Milli-Q water was subtracted from the fluorescence spectrum of the sediment sample to eliminate the Raman scattering peak.<sup>21</sup> Two optical indexes (fluorescence index (FI) and humification index (HIX)) were estimated based on the EEMs measurement.<sup>22–24</sup>

To determine the heavy metals in the sediment samples, the samples were pre-treated by the Lefort *aqua regia* reagent (mixture of nitric acid and hydrochloric acid at volumetric ratio of 3:1), a microwave digestion instrument (Multiprep-41, Milestone, Italy) was then used to digest the samples. Finally, the heavy metals (Cd, Pb, Cu, Zn, Cr, Mn, and Ni) in the sediments were determined using an inductively coupled plasma mass spectrometer (ICAP-RQ, Thermo Fisher, America).

**2.3.3. DNA extraction, PCR amplification and high-throughput sequencing.** The total DNA was extracted from each sediment sample (0.25 g) using the DNeasy PowerSoil kit (QIAGEN, Valencia, CA, USA), according to the manufacturer's instructions. The quality of DNA was assessed by the 1% agarose gel electrophoresis, and the DNA samples were stored at –80 °C until further analysis.

PCR-amplification of the 16S rRNA gene in the sediment DNA extracts was performed using V4 region primers 520F (5'-AYTGGGYDTAAAGNG-3') and 802R (5'-TACNVGGGTATCTA ATCC-3'). The PCR products were detected by electrophoresis in 2% agarose gel and purified with the Agencourt AMPure XP system. The Illumina Hiseq 2500 platform (Illumina Inc., San Diego, CA, USA) was used to sequence the 16S rRNA and the obtained raw sequences were analyzed using QIIME (version 1.9.1). Pair-end reads was merged into a sequence of tags, and the quality of reads and the effect of merge were controlled and filtered. The tags were clustered at 97% similarity level,<sup>25</sup> and RDP classifier<sup>26</sup> was used for the taxonomic assignment of

representative operational taxonomic units (OTU) sequences with the Greengenes as the reference database (version 13.8).<sup>27</sup>

### 2.4. Data processing and analysis

The data in this study are expressed as the means and standard deviations. All the bar charts were drawn using Origin (version 2017, USA). The statistical analysis was performed using IBM SPSS statistics (version 20.0, USA). One-way analysis of variance (ANOVA) followed by least-significant difference (LSD) tests ( $p < 0.05$ ) was carried out to assess the significant differences of physical and chemical parameters among different sections. Principal component analysis (PCA) was used to evaluate the sources of heavy metals. Furthermore, the kriging method was used to draw the horizontal spatial distribution maps of D<sub>50</sub> and heavy metals using Arcgis (version 10.2, USA) software. EEMs optical indexes were resolved by parallel factor analysis (PARAFAC) using MATLAB (version R2015a, USA). Pearson correlation between different parameters of sediment samples were analyzed using the corrplot package in R program (version 4.0.4, New Zealand) and visualized using a heatmap ( $p < 0.05$ ). At the phylum and genus levels, the logarithmic transformation was applied to normalize the data, and the heat maps for the relative abundance of the top 10 dominant bacteria in the sediment samples were drawn using heatmap package in R program (version 4.0.4, New Zealand). The Spearman correlation between the dominant phylum and environmental parameters were analyzed using the corrplot package in R program (version 4.0.4, New Zealand) and visualized using a heatmap ( $p < 0.05$ ).<sup>28</sup>

## 3. Results

### 3.1. Sediment size distribution

The contents of clay (<2 μm), silt (2–50 μm) and sand (50–2000 μm) in the surface sediments of the Linghe Reservoir were 1.07–7.43%, 86.43–93.65% and 4.25–10.92%, respectively. Fig. 2 shows D<sub>50</sub> and particle size frequency distribution curves in different sections. It can be seen clearly that the average value of D<sub>50</sub> at section D (backwater area, 11.85 μm) was the highest. The value slightly decreased from section A (reservoir head, 9.97 μm) to section C (8.32 μm), but the difference was not significant.

### 3.2. Chemical properties of sediments

**3.2.1. Distribution of nutrients and organic matters.** The nutrients and organic matters in the surface sediments of the Linghe Reservoir are presented in Fig. 3. The average concentrations of TN, TP, OM and soluble organic carbon were 3.80 g kg<sup>–1</sup>, 0.89 g kg<sup>–1</sup>, 25.39 g kg<sup>–1</sup> and 0.38 g kg<sup>–1</sup>, respectively. It was obvious that the sediments from the backwater area of the reservoir contained lower amounts of

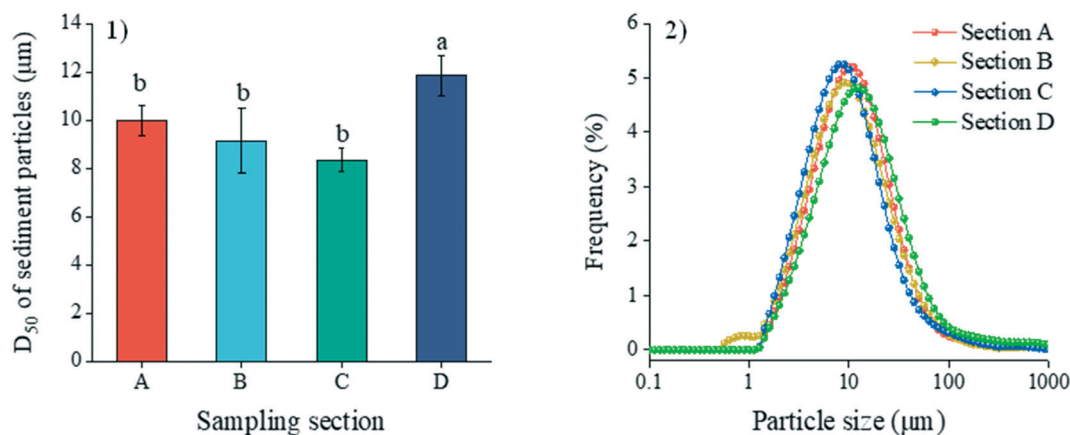


Fig. 2  $D_{50}$  (1) and particle size frequency distribution curves (2). Bars indicate standard deviation of the mean. Different letters above the bars indicate significant differences between sections based on the LSD test ( $p < 0.05$ ).

TN, TP, OM and soluble organic carbon compared to the reservoir head or center area.

**3.2.2. EEM-PARAFAC components and spectral characteristics of DOM.** All the fluorescence EEM spectra of DOM from sediment samples were successfully decomposed into a three-component model by PARAFAC analysis (Fig. 4). The first component (C1;  $\lambda_{Ex/Em} = 235\ 290/414$  nm) was considered as the UVC humic-like substance.<sup>29</sup> The second component (C2;  $\lambda_{Ex/Em} = 275\ 355/474$  nm) was identified as the UVA humic-like substance and its fluorescence

characteristics are similar to that of fulvic acid.<sup>30</sup> The third component (C3;  $\lambda_{Ex/Em} = 225\ 285/298$  nm) was recognized as the tyrosine-like molecules.<sup>31</sup>

Fig. 4 also shows that the difference in the proportions of DOM components at different sampling sections and the distribution trends of FI and HIX. C3 was the main component in the surface sediments of the Linghe Reservoir, accounting for 43.36% on average, compared to 26.86% and 29.78% for C1 and C2, respectively. The FI was in the range of 1.49 to 1.57 for different sampling sections, and the

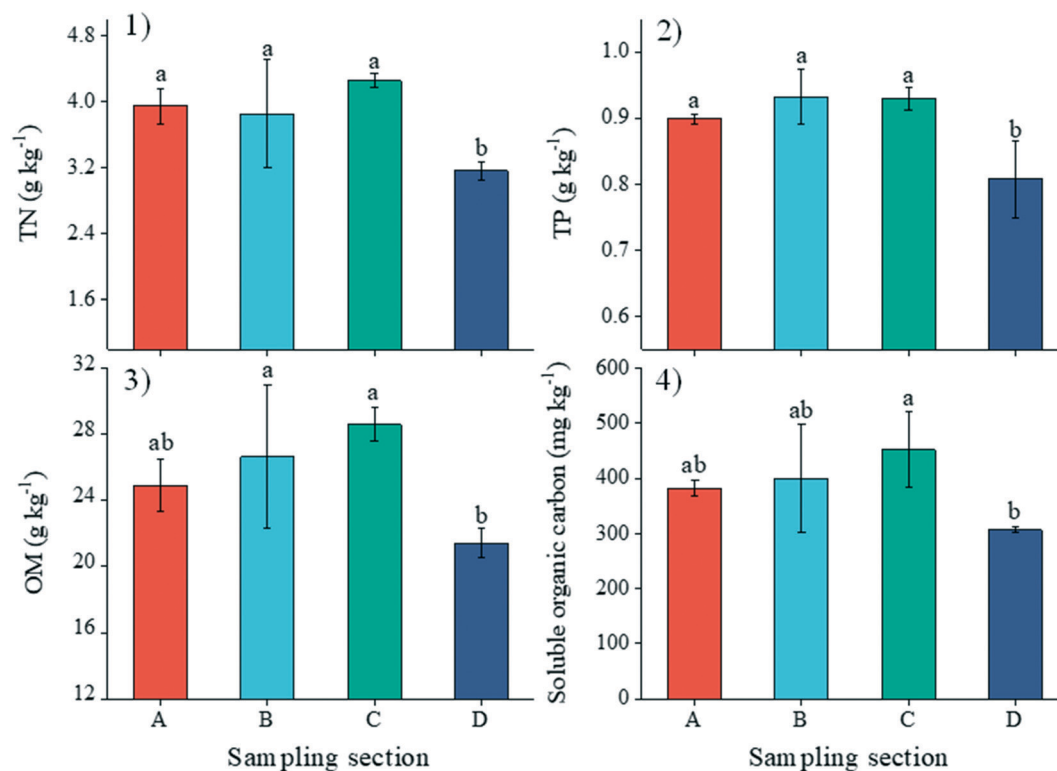


Fig. 3 Chemical properties (1: TN, 2: TP, 3: OM, 4: Soluble organic carbon) of surface sediments from different sections. Bars indicate standard deviation of the mean. Different letters above the bars indicate significant differences between sections based on the LSD test ( $p < 0.05$ ).

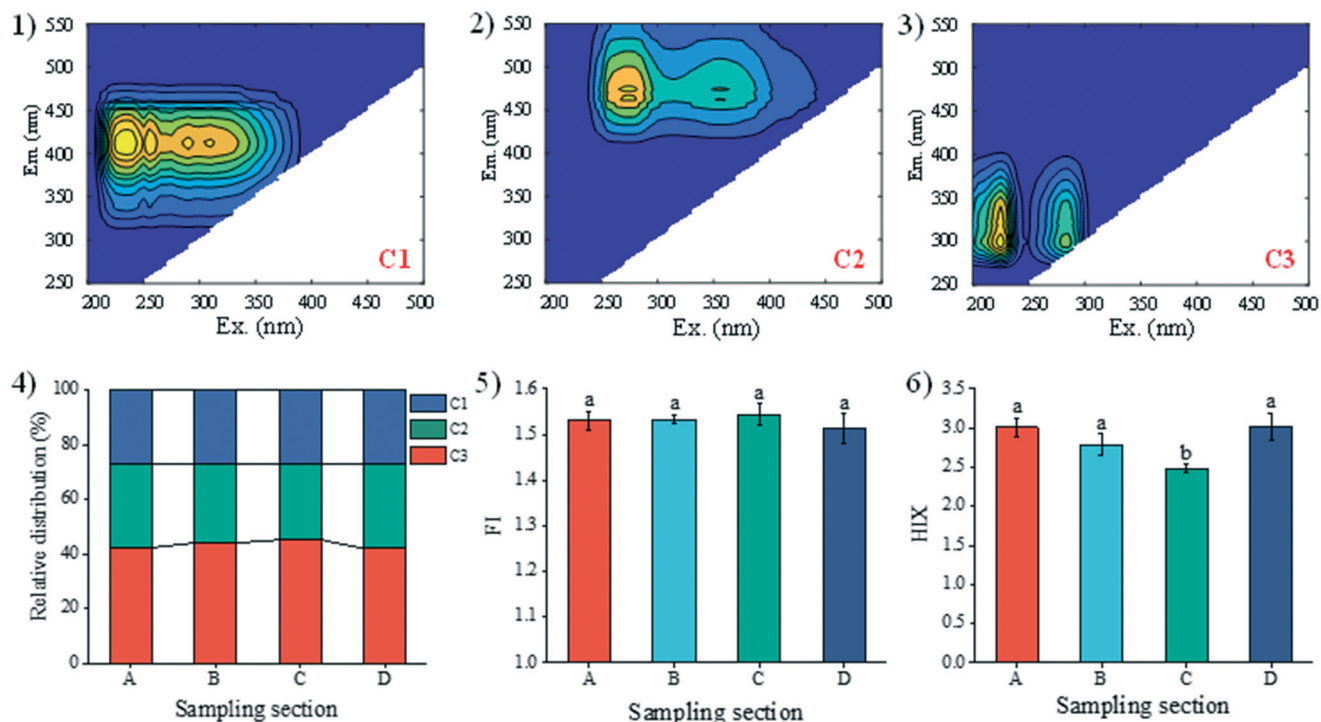


Fig. 4 Three different fluorescence components (1: UVC humic-like, 2: UVA humic-like, 3: tyrosine-like) identified by PARAFAC modeling and optical parameters (4: relative distribution of fluorescence components, 5: fluorescence index, 6: humification index). Bars indicate standard deviation of the mean. Different letters above the bars indicate significant differences between sections based on the LSD test ( $p < 0.05$ ).

difference was not significant. HIX ranged from 2.44 to 3.20, and its distribution trend was similar to that of the sediment particle size.

**3.2.3. Distribution of heavy metals.** The average contents of heavy metals (Cd, Pb, Cu, Zn, Cr, Mn, and Ni) in the surface sediments of the reservoir were  $0.17 \text{ mg Cd kg}^{-1}$ ,  $24.82 \text{ mg Pb kg}^{-1}$ ,  $25.57 \text{ mg Cu kg}^{-1}$ ,  $82.59 \text{ mg Zn kg}^{-1}$ ,  $26.28 \text{ mg Cr kg}^{-1}$ ,  $667.27 \text{ mg Mn kg}^{-1}$  and  $28.95 \text{ mg Ni kg}^{-1}$ , respectively. The maximum contents were  $0.376 \text{ mg Cd kg}^{-1}$ ,  $38.09 \text{ mg Pb kg}^{-1}$ ,  $34.61 \text{ mg Cu kg}^{-1}$ ,  $124.3 \text{ mg Zn kg}^{-1}$ ,  $61.91 \text{ mg Cr kg}^{-1}$ ,  $914.5 \text{ mg Mn kg}^{-1}$ , and  $40.00 \text{ mg Ni kg}^{-1}$ . The spatial distribution patterns of different heavy metals are relatively similar (Fig. 5), with the highest content at the head of the reservoir and lower content at the backwater area and center of the reservoir.

### 3.3. Composition of bacterial communities in sediments

The composition and structure of bacterial communities in the surface sediments of the Linghe Reservoir were analyzed at the phylum and genus levels (Fig. 6). The bacterial communities were dominated by the phylum *Proteobacteria* (34.3%), *Firmicutes* (24.0%), *Bacteroidetes* (17.4%), *Verrucomicrobia* (3.0%), *Actinobacteria* (2.5%), *Cyanobacteria* (2.3%), *Chloroflexi* (2.0%), *OP3* (1.9%), *Chlorobi* (1.8%) and *Acidobacteria* (1.4%), representing more than 90% of total bacterial abundance in the sediments. At the genus level, the bacterial communities were dominated by the genus *Sulfuricurvum* (2.7%), *Arcobacter* (2.3%), *Erysipelothrix* (1.8%),

*Bacteroides* (1.3%), *Coprococcus* (1.3%), *Lactobacillus* (1.1%), *Sedimentibacter* (1.1%), *Parabacteroides* (1.0%), *Clostridium* (1.0%) and *Thiobacillus* (0.9%).

## 4. Discussion

### 4.1. Spatial distribution of sediment particle size

The sediment particle size of the Linghe Reservoir showed a spatial distribution pattern that small particles concentrated in the center of the reservoir and large ones presented at either the head or tail area of the reservoir. When the river flows into the backwater area of a reservoir, the flow velocity slows down and the large sediments deposit. With the gradual decrease of the flow velocity, the sediment particle size also gradually reduces.<sup>32</sup> In the head area of the reservoir, due to the local turbulence caused by flood discharge and the related scouring process, the small particles are suspended and flushed out of the reservoir, the sediment particle size usually increases again.<sup>33-35</sup> The spatial distribution of the sediment particles identified in this study completely agreed with this trend.

### 4.2. Contamination of the sediments

The mean concentrations of TN and TP in the sediments from different sampling sections were evaluated according to the Ontario sediment-quality guidelines (OSQG).<sup>36</sup> As per the OSQG, the lowest effect level (LEL) and the severe effect level (SEL) for TN content are  $0.55 \text{ g kg}^{-1}$  and  $4.80 \text{ g kg}^{-1}$ , respectively. For the TP content, the LEL and SEL are  $0.60 \text{ g}$

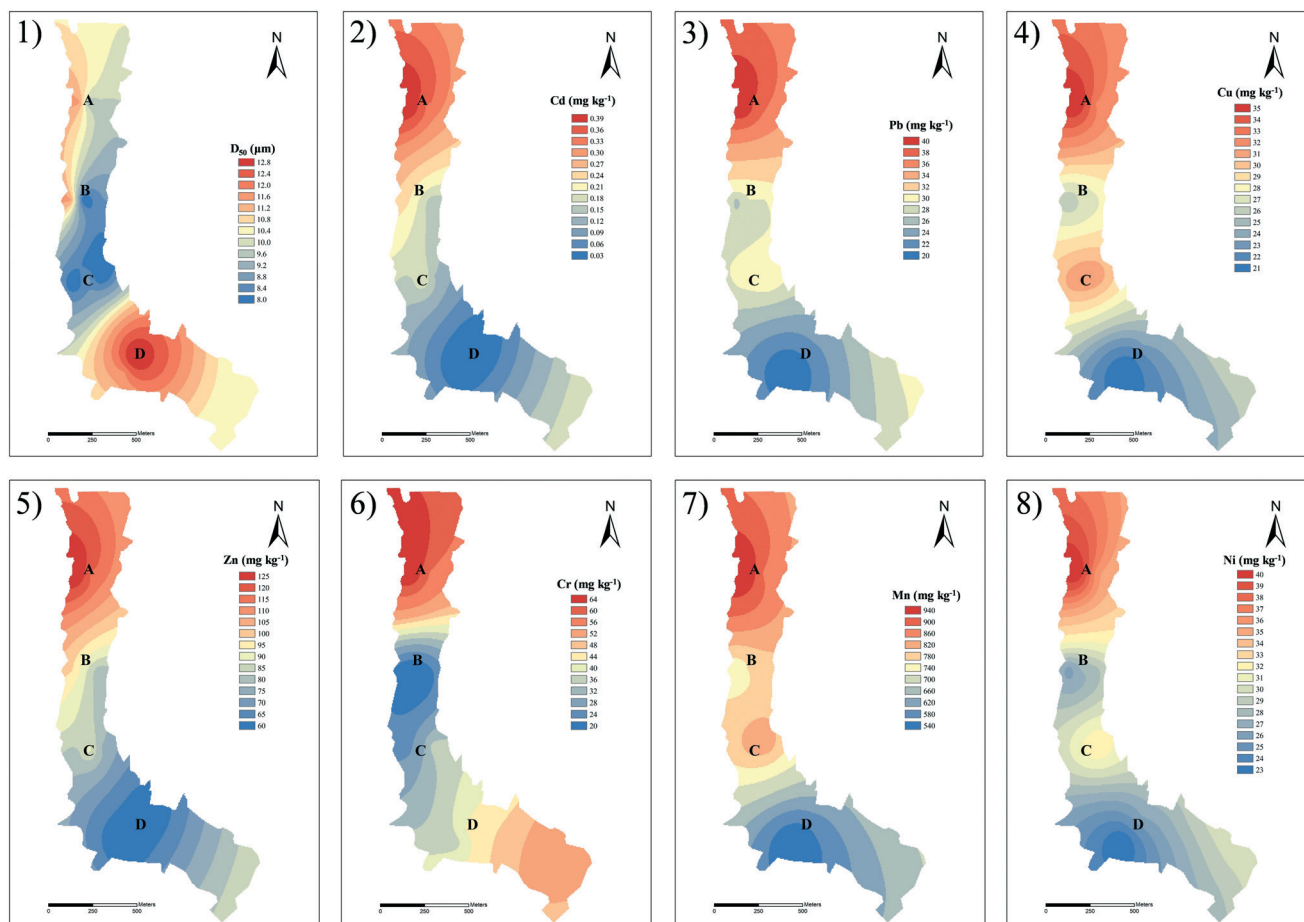


Fig. 5 Spatial distributions of  $D_{50}$  (1) and heavy metals in the sediments (2: Cd, 3: Pb, 4: Cu, 5: Zn, 6: Cr, 7: Mn, and 8: Ni).

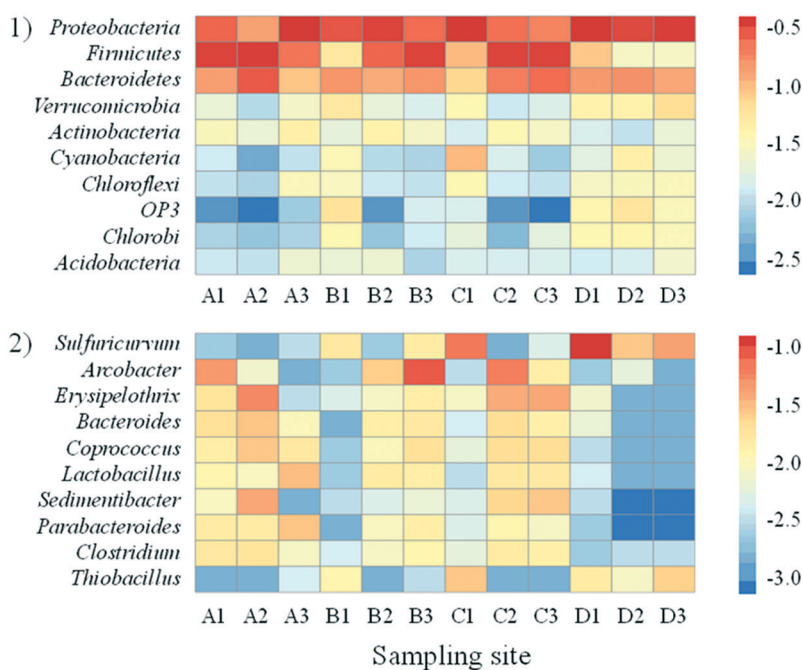


Fig. 6 Heat maps of the relative abundance of dominant phyla (1) and genera (2) in different 6 sediment samples. Bars indicate the relative abundance after logarithmic transformation.

$\text{kg}^{-1}$  and  $2.00 \text{ g kg}^{-1}$ , respectively. When the concentration of TN or TP is lower than the LEL, the sediments are not contaminated; if the concentration of TN or TP is higher than the SEL, the sediments are heavily contaminated. In this study, the TN in the sediments from all sampling sections exceeded the LEL and was close to the SEL. The mean concentration of TP was also above LEL. Therefore, the surface sediments of the Linghe Reservoir was moderately contaminated.

The ratios of the average contents of heavy metals (Cd, Pb, Cu, Zn, Cr, Mn, and Ni) in the surface sediments of the Linghe Reservoir to the background contents of soil elements in China were 1.76 (Cd), 0.95 (Pb), 1.13 (Cu), 1.11 (Zn), 0.43 (Cr), 1.14 (Mn) and 1.08 (Ni), respectively.<sup>37</sup> The geoaccumulation index ( $I_{\text{geo}}$ ) proposed by Muller was used here to assess the heavy metal contamination.<sup>38</sup> It was found that the moderate and slightly Cd contamination existed in section A ( $1 < I_{\text{geo}} \leq 2$ ) and section B ( $0 < I_{\text{geo}} \leq 1$ ), respectively. No other heavy metal (Pb, Cu, Zn, Cr, Mn, and Ni) contamination was identified in the reservoir ( $I_{\text{geo}} \leq 0$ ). The potential ecological risk index proposed by Hakanson<sup>39</sup> was applied to analyze the ecological risk of Cd. The results showed that the potential ecological hazard coefficient of Cd in section A reached a strong ecological hazard level ( $80 \leq E_r^i \leq 160$ ).

Compared with the sediments from other reservoirs in the Yellow River Basin (Table 1), it can be seen that the content of TN of Linghe Reservoir was higher than that of Tangyu Reservoir and Jinpen Reservoir. However, the content of TP from Linghe Reservoir was relatively lower than that of the above two reservoirs. The contents of Cd and Pb were similar to that of Liujiaxia Reservoir. Furthermore, the content of Zn from the Linghe Reservoir was slightly higher than that of Sanmenxia Reservoir, but was significantly lower than that of Liujiaxia Reservoir. The contents of Cu, Cr, Mn and Ni were all lower compared to other reservoirs in the Yellow River Basin. Generally, the TN pollution in the sediments of the Linghe Reservoir was at a relatively high level, but the TP and heavy metals pollutions were at a lower level.

### 4.3. Effect of sediment particle size on the spatial distribution of contaminants

In general, the adsorption capacity of sediments for contaminants is proportional to its specific surface area. The

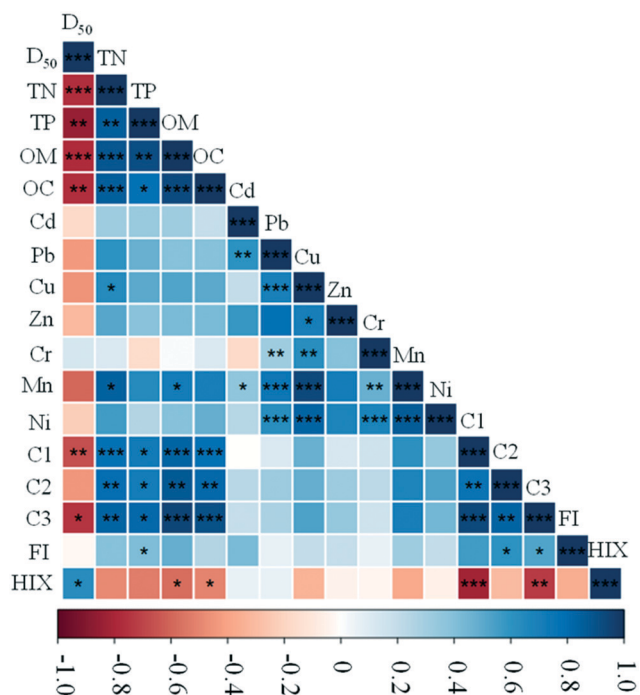


Fig. 7 Pearson correlation heat maps of different environmental parameters (OC refers to soluble organic carbon). Significance levels are shown at  $*p < 0.05$ ,  $**p < 0.01$  and  $***p < 0.001$ .

smaller sediment particle size will result in the larger specific surface area, leading to a better adsorption capacity.<sup>46</sup> Pearson correlation analysis (Fig. 7) demonstrated the significant negative correlations between the sediment particle size and TN, TP, OM and soluble organic carbon in the sediments ( $p < 0.01$ ). This indicated that the horizontal difference in flow velocity led to the natural horizontal distribution of sediment particle size, which further affected the horizontal distributions of organic carbon, nitrogen and phosphorus in sediments directly.

However, there was no significant correlation between  $D_{50}$  and the contents of different heavy metals (Cd, Pb, Cu, Zn, Cr, Mn, and Ni) ( $p > 0.05$ ), indicating that the distributions of heavy metals (Cd, Pb, Cu, Zn, Cr, Mn, and Ni) in the Linghe Reservoir was not affected by the sediment particle size. PCA results (Table 2) demonstrate that the contents of different heavy metals (Cd, Pb, Cu, Zn, Cr, Mn, and Ni) are generalized into two factors, which can explain a relatively large extent of the total variance (88.52%). The first factor

Table 1 Comparisons of TN ( $\text{g kg}^{-1}$ ), TP ( $\text{g kg}^{-1}$ ) and heavy metals ( $\text{mg kg}^{-1}$ ) between Linghe reservoir and other reservoirs in the Yellow River Basin

Reservoir	TN	TP	Cd	Pb	Cu	Zn	Cr	Mn	Ni
Linghe Reservoir	3.80	0.89	0.17	24.82	25.57	82.59	26.28	667.27	28.95
Tangyu Reservoir <sup>40</sup>	2.12	1.37							
Jinpen Reservoir <sup>41</sup>	1.13	1.13							
Liujiaxia Reservoir <sup>42</sup>			0.16	22.44	32.09	291.77	77.03		33.53
Sanmenxia Reservoir <sup>43</sup>			0.10	42.25	47.00	70.20	61.85	1764.25	
Xiaolangdi Reservoir <sup>44</sup>			0.24	47.20	32.03		66.13		
Wangjiaya Reservoir <sup>45</sup>				35.20	41.50	91.20	93.00	892.00	50.30

**Table 2** Principal component loadings and explained variance for two components

Element	PC1	PC2
Cd	0.685	0.560
Pb	0.948	0.056
Cu	0.950	-0.169
Zn	0.644	0.601
Cr	0.829	-0.460
Mn	0.964	-0.099
Ni	0.964	-0.193
Percent of variance	74.75	13.77
Cumulative percent	74.75	88.52

(PC1) explains 74.75% of the total variance, showing the high positive loadings (>0.8) for Pb, Cu, Cr, Mn and Ni. The correlation analysis also shows that there were significant positive correlations ( $p < 0.05$ ) among the Pb, Cu, Cr, Mn and Ni. This indicates that these heavy metals probably had the common sources, mutual dependence, and similar behavior during transport.<sup>47,48</sup> However, the spatial distribution patterns of different heavy metals are relatively similar (Fig. 5) except for Cr. This is probably due to the fact that most of the heavy metals exist as the positive ions, while Cr mainly exists as the negative chromate. Since the contents of these heavy metals (Cd, Pb, Cu, Zn, Cr, Mn, and Ni) in the sediments of the Linghe Reservoir were close to the background contents (0.43–1.14 times), it was considered that the Pb, Cu, Cr, Mn and Ni in the sediments were mainly attributed to the soil erosion. The second factor (PC2) explains 13.77% of the total variance, illustrating the relatively high positive loadings (>0.5) for Cd and Zn. The Cd and Zn in sediment samples were mainly concentrated at the head of the reservoir close to the dam (Fig. 5), therefore, the Zn and Cd in the Linghe Reservoir sediments were likely to

be derived from both soil erosion and local anthropogenic contamination near the dam.

Based on the concentrations and sources of the heavy metals in the sediments of the Linghe Reservoir, it can be suggested that the contents of heavy metals are not the determining factor for the partial desilting implementation.

#### 4.4. Effect of sediment particle size on bacteria

Fig. 8 shows the Spearman correlation between dominant phylum and environmental parameters. The results clearly demonstrated that the *Firmicutes*, *Verrucomicrobia*, and *Chlorobi* were significantly correlated with  $D_{50}$  ( $p < 0.05$ ). On the contrary, these bacterial groups had the strong negative correlations with different environmental parameters, including TN, OM and soluble organic carbon. Although these substances can provide the necessary nutrients for the bacterial communities.

In the backwater area of the Linghe Reservoir, the relative abundance of *Firmicutes* decreased significantly. This is mainly due to the strong degradation capacity and metabolic activity of these bacteria,<sup>49</sup> which make them more widely distributed in areas with high nutrients and organic carbons. In contrast, the relative abundance of *Verrucomicrobia* and *Chlorobi* increased, because these bacteria belong to oligotrophic bacteria and have the strong competitive advantage in areas with low nutrients.<sup>50–52</sup> Since the particle size was negatively correlated with TN, TP, OM and soluble organic carbon (Fig. 7), it was suggested that the sediment particle size indirectly affected the bacterial community structure by influencing the nutrient distribution.

In addition, the sediment particle size also indirectly affected the DOM content released by bacteria. HIX is used to characterize the humification degree of DOM.<sup>53</sup> Smaller HIX indicates a higher endogenous contribution.<sup>54,55</sup> In this study, the smallest HIX was in the section C (Fig. 4), where soluble organic carbon and nutrient concentrations were the highest. This indicated that the bacteria and algae in this section can obtain more required materials (carbon and nutrients), have stronger metabolic activities, and release more active DOM.

#### 4.5. Potential risks of desilting and management strategies

Partial desilting in the section C can effectively reduce the potential endogenous pollution of the Linghe Reservoir. However, the desilting process will cause disturbance of the sediments, which not only results in high turbidity and loss of transparency of overlying water, but also accelerates the release of contaminants from the sediments towards overlying water. Previous study has shown that, after the desilting, the residual sediment particles in the overlying water accounted for 2–11% of the total dredged amount, and the contaminants in the residual particles accounted for approximately 5–9% of contaminants that were planned to be cleaned.<sup>56</sup> These residual sediment particles in the overlying water could take several weeks to be re-settled into the

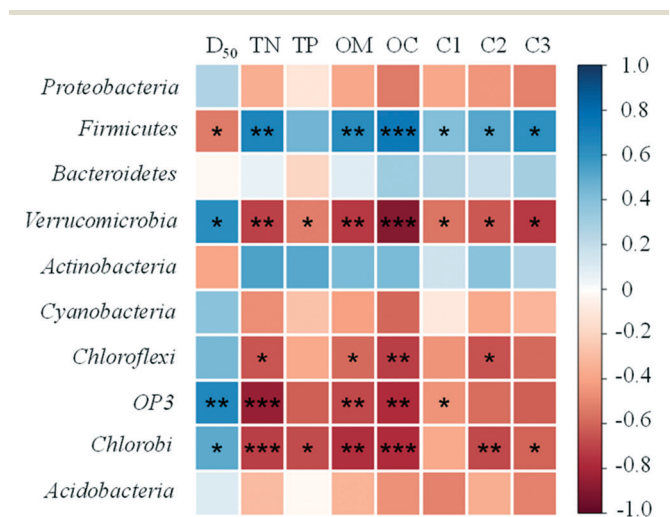


**Fig. 8** Spearman correlation heat maps of dominant phylum and environmental parameters (OC refers to soluble organic carbon). Significance levels are shown at \* $p < 0.05$ , \*\* $p < 0.01$  and \*\*\* $p < 0.001$ .

bottom of the reservoir.<sup>57</sup> This can lead to serious environmental and health risks. For example, the desilting activities can destruct the benthic bacterial community. It may take 2 to 3 years to re-establish the benthic fauna.<sup>58</sup> The nutrients released from the nutrient-laden sediments can promote the algae bloom, leading to the deterioration of water quality and risks to the drinking water supply security.<sup>59,60</sup> Different management strategies can be implemented to mitigate the negative effects of desilting activities, including establishment of specific desilting rate and locations, seasonal desilting restrictions, water quality (turbidity) thresholds, utilization of environmentally-friendly desilting methods, *etc.* With the rigorous planning, careful implementation and close monitoring, the negative effects of desilting activities can be minimized.

## 5. Conclusions

In this study, the effects of sediment particle size on the spatial distributions of contaminants and bacterial communities in the reservoir sediments were investigated. It was identified that the horizontal difference in flow velocity led to the natural horizontal distribution of sediment particle size, which affected the horizontal distributions of organic carbon, nitrogen and phosphorus in sediments directly. It further indirectly affected the bacterial community structure and the DOM content released by the bacteria. Our results also showed that the heavy metals (Cd, Pb, Cu, Zn, Cr, Mn, and Ni) were mainly concentrated in the reservoir head, which had no significant correlation with the sediment particle size.

## Conflicts of interest

There are no conflicts to declare.

## References

- 1 Y. Ding, M. Li, B. Pan, G. Zhao and L. Gao, Disentangling the drivers of phytoplankton community composition in a heavily sediment-laden transcontinental river, *J. Environ. Manage.*, 2022, **302**, 113939.
- 2 H. Chanson and D. James, Siltation of Australian reservoirs: some observations and dam safety implications, *Proceedings of the 28th IAHR Congress*, 1999.
- 3 T. Dalu, E. M. Tambara, B. Clegg, L. D. Chari and T. Nhwatiwa, Modeling sedimentation rates of Malilangwe reservoir in the south-eastern lowveld of Zimbabwe, *Appl. Water Sci.*, 2013, **3**, 133–144.
- 4 C. Tundu, M. J. Tumbare and J.-M. Kileshye Onema, Sedimentation and its impacts/effects on river system and reservoir water quality: case study of Mazowe catchment, Zimbabwe, *Proc. Int. Assoc. Hydrol. Sci.*, 2018, **377**, 57–66.
- 5 S. Rice, Which tributaries disrupt downstream fining along gravel-bed rivers?, *Geomorphology*, 1998, **22**, 39–56.
- 6 X. Liu, Z. Li, P. Li, B. Zhu, F. Long, Y. Cheng, T. Wang and K. Lu, Changes in carbon and nitrogen with particle size in bottom sediments in the Dan River, China, *Quat. Int.*, 2015, **380**, 305–313.
- 7 P. M. Mwanamoki, N. Devarajan, F. Thevenon, N. Birane, L. F. de Alencastro, D. Grandjean, P. T. Mpiana, K. Prabakar, J. I. Mubedi, C. G. Kabele, W. Wildi and J. Poté, Trace metals and persistent organic pollutants in sediments from river-reservoir systems in Democratic Republic of Congo (DRC): Spatial distribution and potential ecotoxicological effects, *Chemosphere*, 2014, **111**, 485–492.
- 8 A. Yazidi, S. Saidi, N. Ben Mbarek and F. Darragi, Contribution of GIS to evaluate surface water pollution by heavy metals: Case of Ichkeul Lake (Northern Tunisia), *J. Afr. Earth Sci.*, 2017, **134**, 166–173.
- 9 A. A. Al-Taani, A. T. Batayneh, N. El-Radaideh, H. Ghrefat, T. Zumlot, A. M. Al-Rawabdeh, T. Al-Momani and A. Taani, Spatial distribution and pollution assessment of trace metals in surface sediments of Ziqlab Reservoir, Jordan, *Environ. Monit. Assess.*, 2015, **187**, 32.
- 10 A. C. Torregroza-Espinosa, E. Martínez-Mera, D. Castañeda-Valbuena, L. C. González-Márquez and F. Torres-Bejarano, Contamination Level and Spatial Distribution of Heavy Metals in Water and Sediments of El Guájaro Reservoir, Colombia, *Bull. Environ. Contam. Toxicol.*, 2018, **101**, 61–67.
- 11 A. K. Singh, S. I. Hasnain and D. K. Banerjee, Grain size and geochemical partitioning of heavy metals in sediments of the Damodar River – a tributary of the lower Ganga, India, *Environ. Geol.*, 1999, **39**, 90–98.
- 12 D. E. Walling and P. W. Moorehead, The particle size characteristics of fluvial suspended sediment: an overview, *Hydrobiologia*, 1989, **176**, 125–149.
- 13 L. Liu, F. Li, D. Xiong and C. Song, Heavy metal contamination and their distribution in different size fractions of the surficial sediment of Haihe River, China, *Environ. Geol.*, 2006, **50**, 431–438.
- 14 L. Wang, L. Liu, B. Zheng, Y. Zhu and X. Wang, Analysis of the bacterial community in the two typical intertidal sediments of Bohai Bay, China by pyrosequencing, *Mar. Pollut. Bull.*, 2013, **72**, 181–187.
- 15 J. A. Santmire and L. G. Leff, The influence of stream sediment particle size on bacterial abundance and community composition, *Aquat. Ecol.*, 2007, **41**, 153–160.
- 16 B. Zheng, L. Wang and L. Liu, Bacterial community structure and its regulating factors in the intertidal sediment along the Liaodong Bay of Bohai Sea, China, *Microbiol. Res.*, 2014, **169**, 585–592.
- 17 P. López, J. A. López-Tarazón, J. P. Casas-Ruiz, M. Pompeo, J. Ordoñez and I. Muñoz, Sediment size distribution and composition in a reservoir affected by severe water level fluctuations, *Sci. Total Environ.*, 2016, **540**, 158–167.
- 18 M. Li, W. Zhu and L. Gao, Analysis of Cell Concentration, Volume Concentration, and Colony Size of Microcystis Via Laser Particle Analyzer, *Environ. Manage.*, 2014, **53**, 947–958.
- 19 M. Li, L. Gao and L. Lin, Specific growth rate, colonial morphology and extracellular polysaccharides (EPS) content of *Scenedesmus obliquus* grown under different levels of light limitation, *Int. J. Oceanol. Limnol.*, 2015, **51**, 329–334.

- 20 S. Bao, *Soil and agricultural chemistry analysis*, China agriculture press, Beijing, 2000.
- 21 M. Wei, C. Gao, Y. Zhou, P. Duan and M. Li, Variation in spectral characteristics of dissolved organic matter in inland rivers in various trophic states, and their relationship with phytoplankton, *Ecol. Indic.*, 2019, **104**, 321–332.
- 22 R. M. Cory and D. M. McKnight, Fluorescence Spectroscopy Reveals Ubiquitous Presence of Oxidized and Reduced Quinones in Dissolved Organic Matter, *Environ. Sci. Technol.*, 2005, **39**, 8142–8149.
- 23 T. Ohno, Fluorescence Inner-Filtering Correction for Determining the Humification Index of Dissolved Organic Matter, *Environ. Sci. Technol.*, 2002, **36**, 742–746.
- 24 Z. Ge, L. Gao, N. Ma, E. Hu and M. Li, Variation in the content and fluorescent composition of dissolved organic matter in soil water during rainfall-induced wetting and extract of dried soil, *Sci. Total Environ.*, 2021, **791**, 148296.
- 25 R. C. Edgar, Search and clustering orders of magnitude faster than BLAST, *Bioinformatics*, 2010, **26**, 2460–2461.
- 26 Q. Wang, G. M. Garrity, J. M. Tiedje and J. R. Cole, Naive Bayesian classifier for rapid assignment of rRNA sequences into the new bacterial taxonomy, *Appl. Environ. Microbiol.*, 2007, **73**, 5261–5267.
- 27 T. Z. DeSantis, P. Hugenholtz, N. Larsen, M. Rojas, E. L. Brodie, K. Keller, T. Huber, D. Dalevi, P. Hu and G. L. Andersen, Greengenes, a chimera-checked 16S rRNA gene database and workbench compatible with ARB, *Appl. Environ. Microbiol.*, 2006, **72**, 5069–5072.
- 28 C. Chang, L. Gao and J. Wei, *et al.*, Spatial and environmental factors contributing to phytoplankton biogeography and biodiversity in mountain ponds across a large geographic area, *Aquat. Ecol.*, 2021, **55**, 721–735.
- 29 C. A. Stedmon and S. Markager, Resolving the variability in dissolved organic matter fluorescence in a temperate estuary and its catchment using PARAFAC analysis, *Limnol. Oceanogr.*, 2005, **50**, 686–697.
- 30 C. A. Stedmon, S. Markager and R. Bro, Tracing dissolved organic matter in aquatic environments using a new approach to fluorescence spectroscopy, *Mar. Chem.*, 2003, **82**, 239–254.
- 31 P.-Q. Fu, C.-Q. Liu and F.-C. Wu, Three-dimensional excitation emission matrix fluorescence spectroscopic characterization of dissolved organic matter, *Spectrosc. Spectral Anal.*, 2005, **25**, 2024–2028.
- 32 Q. Tang, A. L. Collins, A. Wen, X. He, Y. Bao, D. Yan, Y. Long and Y. Zhang, Particle size differentiation explains flow regulation controls on sediment sorting in the water-level fluctuation zone of the Three Gorges Reservoir, China, *Sci. Total Environ.*, 2018, **633**, 1114–1125.
- 33 W. Yu, L. Yuntao and F. Qi, Effects of dam interception on the spatial distribution of sediment granularities in Heihe River, *J. Lake Sci.*, 2019, **31**, 1459–1467.
- 34 X. Xia, J. Dong, M. Wang, H. Xie, N. Xia, H. Li, X. Zhang, X. Mou, J. Wen and Y. Bao, Effect of water-sediment regulation of the Xiaolangdi reservoir on the concentrations, characteristics, and fluxes of suspended sediment and organic carbon in the Yellow River, *Sci. Total Environ.*, 2016, **571**, 487–497.
- 35 J. Huang, X. Ge, X. Yang, B. Zheng and D. Wang, Remobilization of heavy metals during the resuspension of Liangshui River sediments using an annular flume, *Chin. Sci. Bull.*, 2012, **57**, 3567–3572.
- 36 D. Persaud, R. Jaagumagi and A. Hayton, *Guidelines for the protection and management of aquatic sediment quality in Ontario*, Ontario Ministry of the Environment, Toronto, 1993.
- 37 F. Wei, C. Zheng, J. Chen and Y. Wu, Study on the background contents on 61 elements of soils in China, *Environ. Sci.*, 1991, **12**, 12–19.
- 38 G. Muller, Index of geoaccumulation in sediments of the Rhine River, *Geojournal*, 1969, **2**, 108–118.
- 39 L. Hakanson, An ecological risk index for aquatic pollution control. a sedimentological approach, *Water Res.*, 1980, **14**, 975–1001.
- 40 T. Huang, S. Yan, B. Chai and H. Liu, Phosphorus Forms and Its Distribution in Source Water Reservoir Sediment, *Tianjin Keji Daxue Xuebao*, 2011, **44**, 607–612.
- 41 E. Pop, V. Varshney and A. K. Roy, Thermal properties of graphene: Fundamentals and applications, *MRS Bull.*, 2012, **37**, 1273–1281.
- 42 M. E. A. Ali, L. Wang, X. Wang and X. Feng, Thin film composite membranes embedded with graphene oxide for water desalination, *Desalination*, 2016, **386**, 67–76.
- 43 Q. Cheng, R. Wang, W. Huang, W. Wang and X. Li, Assessment of heavy metal contamination in the sediments from the Yellow River Wetland National Nature Reserve (the Sanmenxia section), China, *Environ. Sci. Pollut. Res.*, 2015, **22**, 8586–8593.
- 44 T. Liu, B. Yang, N. Graham, W. Yu and K. Sun, Trivalent metal cation cross-linked graphene oxide membranes for NOM removal in water treatment, *J. Membr. Sci.*, 2017, **542**, 31–40.
- 45 Y. Oh, D. L. Armstrong, C. Finnerty, S. Zheng, M. Hu, A. Torrents and B. Mi, Understanding the pH-responsive behavior of graphene oxide membrane in removing ions and organic micropollutants, *J. Membr. Sci.*, 2017, **541**, 235–243.
- 46 S. Wang, X. Jin, Q. Bu, X. Zhou and F. Wu, Effects of particle size, organic matter and ionic strength on the phosphate sorption in different trophic lake sediments, *J. Hazard. Mater.*, 2006, **128**, 95–105.
- 47 A. Baran, M. Tarnawski and T. Koniarczyk, Spatial distribution of trace elements and ecotoxicity of bottom sediments in Rybnik reservoir, Silesian-Poland, *Environ. Sci. Pollut. Res.*, 2016, **23**, 17255–17268.
- 48 G. Suresh, P. Sutharsan, V. Ramasamy and R. Venkatachalapathy, Assessment of spatial distribution and potential ecological risk of the heavy metals in relation to granulometric contents of Veeranam lake sediments, India, *Ecotoxicol. Environ. Saf.*, 2012, **84**, 117–124.
- 49 G. Szabó, B. Khayer, A. Ruzsnyák, I. Tátrai, G. Dévai, K. Márialigeti and A. K. Borsodi, Seasonal and spatial

- variability of sediment bacterial communities inhabiting the large shallow Lake Balaton, *Hydrobiologia*, 2011, **663**, 217–232.
- 50 I. V. Senechkin, A. G. C. L. Speksnijder, A. M. Semenov, A. H. C. van Bruggen and L. S. van Overbeek, Isolation and Partial Characterization of Bacterial Strains on Low Organic Carbon Medium from Soils Fertilized with Different Organic Amendments, *Microb. Ecol.*, 2010, **60**, 829–839.
- 51 U. N. da Rocha, F. D. Andreote, J. L. de Azevedo, J. D. van Elsas and L. S. van Overbeek, Cultivation of hitherto-uncultured bacteria belonging to the Verrucomicrobia subdivision 1 from the potato (*Solanum tuberosum* L.) rhizosphere, *J. Soils Sediments*, 2010, **10**, 326–339.
- 52 W. Hongyue, Y. Jingli, L. Qianxue, M. Qiaoli, W. Terigele, X. Yaru, L. Jingjing and Z. He, Ji and Xininigen, Spatial distribution characteristics of soil microbial communities from Chlorobi phylum in different vegetation zones from Xilin River Basin, *Acta Microbiol. Sin.*, 2021, **61**, 1698–1714.
- 53 T. Ohno, I. J. Fernandez, S. Hiradate and J. F. Sherman, Effects of soil acidification and forest type on water soluble soil organic matter properties, *Geoderma*, 2007, **140**, 176–187.
- 54 Y. Zhang, E. Zhang, Y. Yin, M. A. van Dijk, L. Feng, Z. Shi, M. Liu and B. Qina, Characteristics and sources of chromophoric dissolved organic matter in lakes of the Yungui Plateau, China, differing in trophic state and altitude, *Limnol. Oceanogr.*, 2010, **55**, 2645–2659.
- 55 A. Huguet, L. Vacher, S. Relexans, S. Saubusse, J. M. Froidefond and E. Parlanti, Properties of fluorescent dissolved organic matter in the Gironde Estuary, *Org. Geochem.*, 2009, **40**, 706–719.
- 56 National Research Council, *Sediment Dredging at Superfund Megsites: Assessing the Effectiveness*, The National Academies Press, Washington, DC, 2007, DOI: 10.17226/11968.
- 57 J. Eggleton and K. V. Thomas, A review of factors affecting the release and bioavailability of contaminants during sediment disturbance events, *Environ. Int.*, 2004, **30**, 973–980.
- 58 R. Carline and O. Brynildson, Effects of hydraulic dredging on the ecology of native trout populations in Wisconsin spring ponds, *Technical Bulletin - Wisconsin Department of Natural Resources*, 1977.
- 59 W. Zhu, X. Zhou, H. Chen, L. Gao, M. Xiao and M. Li, High nutrient concentration and temperature alleviated formation of large colonies of Microcystis: Evidence from field investigations and laboratory experiments, *Water Res.*, 2016, **101**, 167–175.
- 60 S. Ye, L. Gao, A. Zamyadi, C. M. Glover, N. Ma, H. Wu and M. Li, Multi-proxy approaches to investigate cyanobacteria invasion from a eutrophic lake into the circumjacent groundwater, *Water Res.*, 2021, **204**, 117578.